Eur. Phys. J. C manuscript No.
(will be inserted by the editor)

Bag model of hadrons, dual QCD thermodynamics and Quark-Gluon Plasma

H. C. Chandola[a,1], **Garima Punetha**[b,1], **H. Dehnen**[c,2]

[1]Department of Physics, Kumaun University, Nainital-263002, India
[2]Fachbereich Physik, Universität Konstanz, M 677, 78457 Konstanz, Germany

arXiv:1501.01153v2 [hep-ph] 11 Mar 2015

Received: date / Accepted: date

Abstract Using the grand canonical ensemble formulation of a multi-particle statistical system, the thermodynamical description of the dual QCD has been presented in terms of the bag model of hadrons and analyzed for the quark-gluon plasma phase of hadronic matter. The dual QCD bag construction has been shown to lead to the radial pressure on the bag surface in terms of the vector glueball masses of the magnetically condensed QCD vacuum. Constructing the grand canonical partition function to deal with the quark-gluon plasma phase of the non-strange hadrons, the energy density and the plasma pressure have been derived and used to understand the dynamics of the associated phase transition. The critical temperature for QGP-hadron phase transition has been derived and numerically estimated by using various thermodynamic considerations. A comparison of the values of the critical temperatures for QGP-hadron phase transition with those obtained for the deconfinement-phase transition, has been shown to lead to the relaxation of the system via a mixed phase of QGP and hot hadron gas. The associated profiles of the normalized energy density and the specific heat have been shown to lead to a huge latent heat generation and indicate the onset of a first-order QGP phase transition. The squared speed of sound has been shown to act as a physical measure of large thermodynamical fluctuations near transition point where it shows a large reduction in its value as compared to the conformal limit and has intimate connection with the evolution of fire-ball and QGP in heavy-ion collision events. The possible implications of the trace anomaly and conformal measure on QGP formation have also been discussed and a considerable increase in the degrees of freedom and the associated interaction effects has been indicated around the transition region. The various physical parameters analyzed here have been shown to lead to a reliable physical picture of the QGP phase transition which have a deep relevance with the modern high energy heavy-ion collision experiments aimed at the possibility to explore the new high energy state of matter consisting of the interacting quarks and gluons.

1 Introduction

The development and subsequent applications of the field theoretical methods at finite temperature and non-zero chemical potential, has been boosted recently by the concepts of current heavy ion experiments with Ultra-relativistic energies at the modern heavy ion colliders like RHIC and LHC which are designed to create an entirely new form of matter, called the quark-gluon plasma (QGP)[1–6]. In fact, such experimental and the associated theoretical investigations are of crucial importance, not only for the search of the QGP [7–9] but for the detailed study of the phase transitions in QCD also. However, the progress in the understanding of the properties of the QGP is still elusive mainly because of two reasons: first, the low energy QCD is highly non-perturbative in nature and second, the experimental data are hard to analyse and quantify in infrared sector. Even then, the phase transitions between hadronic matter and the quark-gluon plasma are of extreme interest since they play important role not only in QCD domain of particle physics but also in the evolutionary scenario of early universe in astrophysics and cosmology. Though, one of the tool to analyse the nature of such quark-hadron phase transitions, is the perturbative QCD which is applicable at high temperatures and pressures [10], it exhibits infrared singularities complicating the quantitative analysis close to the transition temperature. Furthermore, the lattice gauge theories have also been developed using the finite temperature QCD and have contributed

[a]chandolaharish@gmail.com
[b]garimapunetha@gmail.com
[c]Heinz.Dehnen@uni-konstanz.de

a lot in understanding the phase transitions by providing the value of critical temperature, the order of the phase transition and the temperature dependence of the bulk thermodynamic quantities such as the pressure or the energy density of the matter. Hence, the lattice QCD as an another alternative tool, may in principle be applicable close to the transition temperature [11–18]. However, it requires a large amount of computer time when dynamical fermions are included and the non-zero baryon chemical potential is incorporated. Furthermore, another largely used model is that related to the relativistic hydrodynamics where, in addition to the energy momentum conservation, one needs an equation of state (EOS) for the QGP. One EOS mostly used is that of a massless relativistic non-interacting gas of quarks and gluons and the non-perturbative confinement is accounted by the bag constant. The lattice results for the QGP, however, indicate that the plasma shows a non ideal or non-perturbative behavior even at the temperatures close to the transition temperature and the above-mentioned EOS does not agree with the lattice results. On the other hand, various experiments on relativistic nuclear collisions are definitely aimed to unfold the entirely different QGP phase transition in various different ways [19, 20]. It is expected that a QGP thus formed will hadronize via formation of a mixed phase of dense plasma and a dilute hadron gas (HG). Since, the specific entropy per baryon during a first-order phase transition is always larger in a QGP phase then that in a hadron gas (HG) phase; using Gibbs criteria for a phase equilibrium, one can generate a phase transition from a QGP to the HG phase for which the specific entropy per baryon always decreases across the phase boundary [21–28]. Since the change of a state is thermodynamically possible at either increasing or a constant entropy, a modification in the values of the temperature and baryon chemical potential is naturally desired during the hadronization of the QGP. An equation of state for the QGP phase has also been proposed [29] using a temperature and chemical potential dependent bag constant in an isentropic equilibrium phase transition from QGP to HG phase, as a result of which the specific entropy per baryon becomes continuous across the phase boundary. The hadronic phase has been treated in this model as a gas of massless pions and massive nucleons and a hard-core repulsion is introduced between a pair of nucleons for incorporating the finite size effects of the baryons in HG phase. However, the detailed analysis of the model for the nature of a temperature and chemical potential dependent bag constant leads to an anomalous behavior[30, 31].

In the present paper, using the grand canonical ensemble formulation of a multi-particle statistical system, the thermodynamic description of the dual QCD has been presented in terms of the bag model of hadrons and analysed for the quark-gluon plasma phase of hadronic matter. Utilizing the thermodynamical concepts for the understanding of the phase transitions and the other thermal effects in dual QCD, the thermodynamical potential has been constructed in terms of the partition function of the grand canonical ensemble formalism and used for the identification of some of the important thermodynamical variables. The thermodynamical potential for the fermions and bosons has been calculated separately in terms of the temperature and chemical potential variables and used for the description of mesonic and baryonic forms of the hadrons. Constructing the bag model for hadrons using the confining part of the energy in our dual QCD formulation, the minimization of the energy of the spherical bag has been used to calculate the effective radius of the bag and the radial pressure on the bag surface which has been shown to depend on the vector glueball masses of magnetically condensed QCD vacuum. Constructing the grand canonical partition function for the quark-gluon plasma phase of the non-strange hadrons, the energy density and the plasma pressure are derived and used to understand the dynamics of phase transition. In case of the baryon free matter, for a simplest system of pions (mesonic system with the vanishing the chemical potential), the energy density, entropy density and pressure are evaluated for hadronic as well as plasma phases, which have been used to derive the expression for the transition temperature by using Gibbs criteria for hadron-QGP phase transition. In an identical way, the analysis has been extended to the case of baryonic matter with finite chemical potential, for which the hadron pressure has been evaluated and used to derive the expression for the critical temperature of hadron-QGP phase transition by incorporating the Gibbs criteria. The numerical estimation of the associated critical temperature of phase transition then leads to the values identical to those obtained using the chemical potential plots in the full infrared sector of QCD. Moreover, the values of the QGP-hadron phase transition temperatures, thus obtained in mesonic and baryonic cases, have been shown to be in a good agreement with each other. A comparison of the values of the critical temperatures for QGP-hadron phase transition with those obtained for the deconfinement phase transition[32], has been shown to lead the relaxation of the system via a mixed phase of QGP and hot hadron gas.

The normalised energy density and specific heat at constant volume have been analyzed for their temperature dependence which has been shown to lead to the generation of a large amount of latent heat and indicate the onset of a first order QGP phase transition. The large specific heat as well as latent heat at the transition point thus have been shown to act as a measure of the large energy fluctuations and the possible signals for QGP. Similarly, the squared speed of sound taken as a kinetic variable has been shown to act as an another measure of the large thermodynamical fluctuations near transition point governing the flow properties of QGP and the evolution of fire-ball in heavy-ion collisions.

The computation of trace anomaly has been shown to lead to the high interaction measure and considerable interaction effects close to the transition region which pushes the associated QGP system far away from the conformal limit. On the other hand, the computation of the conformal measure has been shown to lead its thermal response just complementary to that of the squared sound speed and indicate the breakdown of the conformal symmetry till the transition point for QGP is reached. The thermal response of the trace anomaly and conformal measure has been shown to lead an increasing conformal behavior of QGP at higher temperatures beyond the transition point. The physical relevance of all these thermodynamic parameters has also been discussed in view of the various on going experimental programmes of heavy-ion collision experiments.

2 Review of Dual QCD with Magnetic Symmetry

The nonperturbative features of color gauge theory become more transparent when we express it in a dual form and analyse its underlying feature for the possible dual dynamics between color isocharges and topological charges. A gauge symmetry (G), in fact, may be visualized as a $n-$dimensional isometry in the higher-dimensional unified metric formulation of the gauge theory where the unified space P may be identified as a $(4+n)-$dimensional metric manifold g_{AB} $(A,B=0,1,2\cdots 3+n)$. With the identification of the quotient space P/G as the base manifold (four-dimensional space-time M) and G as a structure group, the unified space may be regarded as a principal fibre bundle $P(M,G)$ over space-time with a canonical projection $\Pi :\rightarrow M$. As a result, the Killing vector fields (ξ_i) associated with the $n-$dimensional isometric group (G) become the fundamental vector fields which generate the right action of G on P and reduce the integral manifold of Killing vectors to a vertical fiber. A connection on $P(M,G)$, thus, admits a left isometry H which formally forms a subgroup of G (the right isometry) and commutes with it. Magnetic symmetry [33–35] may then be introduced as an additional internal isometry H which is the Cartan's subgroup of G and admits some additional Killing vector fields $(m_a;\ a=1,\cdots k=dim\ H)$ in the resulting gauge theory such that,

$$m_a = m_a^i \xi_i,\ \ [m_a,\xi_i\,]=0,\ \ [\xi_i,\xi_j]=f_{ijk}\,\xi_k$$

and

$$\mathscr{L}_{m_a} g_{AB} = 0, \tag{1}$$

as the condition for the Lie derivative along m_a. The magnetic symmetry, which restricts the connection to those whose holonomy bundle becomes a reduced bundle as a result of the killing condition (1), may then be introduced in terms of the gauge-covarient condition given by,

$$D_\mu \hat{m} = 0\,,\ i.e.\ \ (\partial_\mu + g\,\mathbf{W}_\mu \times\,)\hat{m} = 0\,, \tag{2}$$

where $\hat{m}$ is a scalar multiplet which belongs to the adjoint representation of the gauge group G. Consequently, the symmetry of the multiplet becomes the symmetry of the potentials and the monopole emerges as a topological object associated with the elements of the second homotopic group $\Pi_2(G/H)$. The equation (2) then yields an exact solution for the gauge potential for the simplest choice of $G\equiv SU(2)$ gauge symmetry (with H as its little group $U(1)$) as given below,

$$\mathbf{W}_\mu = A_\mu\,\hat{m} - g^{-1}\,(\hat{m}\times\partial_\mu\,\hat{m})\,, \tag{3}$$

where, $A_\mu \equiv \hat{m}\cdot\mathbf{W}_\mu$ is the color electric part unrestricted by the magnetic symmetry. On the other hand, the second part which is determined completely by the magnetic symmetry, is of topological origin since the multiplet $\hat{m}$ may be viewed to define the homotopy of the mapping $\Pi_2\,(S^2)$ as, $\hat{m}:\,S^2_R \rightarrow S^2 = SU(2)/U(1)$, which identifies the point-like monopoles of the non-Abelian symmetry. Thus, the field strength associated with the gauge potential (3) may be expressed as,

$$\mathbf{G}_{\mu\nu} = \mathbf{W}_{\nu,\mu} - \mathbf{W}_{\mu,\nu} + g\,(\mathbf{W}_\mu\times\mathbf{W}_\nu) \equiv (\,F_{\mu\nu} + B^{(d)}_{\mu\nu}\,)\,\hat{m}\,, \tag{4}$$

where, $F_{\mu\nu} = A_{\nu,\mu} - A_{\mu,\nu}$ and $B^{(d)}_{\mu\nu} = -\,g^{-1}\,\hat{m}\cdot(\,\partial_\mu\hat{m}\times\partial_\nu\hat{m})$. The topological structure of the theory may then be brought into dynamics explicitly when such separation of the gauge fields is performed in the magnetic gauge obtained by rotating $\hat{m}$ to a prefixed direction in isospace using a gauge transformation (U) as, $\hat{m}\xrightarrow{U}\xi_3 = (0,\ 0,\ 1)^T$. Using the simplest parametrization for $\hat{m}$ as, $\hat{m} = (\sin\alpha\cos\beta,\ \sin\alpha\sin\beta,\ \cos\alpha)^T$ and choosing $U = \exp\,(-\,\alpha\,t_2 - \beta\,t_3)$, the gauge potential and the gauge field strength, in magnetic gauge are obtained in their simple form as,

$$\mathbf{W}_\mu \xrightarrow{U} (A_\mu + B_\mu)\,\hat{\xi}_3\,, and\ \ \mathbf{G}_{\mu\nu}\xrightarrow{U}(\,F_{\mu\nu} + B^{(d)}_{\mu\nu}\,)\,\hat{\xi}_3\,, \tag{5}$$

where,

$$B_\mu = g^{-1}\,cos\,\alpha\,\partial_\mu\beta$$

$$B^{(d)}_{\mu\nu} = -\,g^{-1}\,\sin\alpha\,(\alpha_{,\mu}\,\beta_{,\nu} - \alpha_{,\nu}\,\beta_{,\mu}) \equiv B_{\nu,\mu} - B_{\mu,\nu}. \tag{6}$$

The part B_μ, fixed completely by $\hat{m}$, is thus identified as the magnetic potential associated with the topological monopoles and therefore the topological properties of $\hat{m}$ are brought down to a dynamical variable (B_μ) by removing all non-essential gauge degrees of freedom of the original gauge symmetry. The fields, thus, appear in a completely dual symmetric way and induce a dual dynamics between color isocharges and topological charges. This is clearly evident if we use the $SU(2)$ Lagrangian with a quark doublet source $\psi(x)$ as,

$$\pounds = -\,\frac{1}{4}\,\mathbf{G}^2_{\mu\nu} + \bar{\psi}(x)\,i\,\gamma^\mu\,D_\mu\,\psi(x) - m_0\,\bar{\psi}(x)\,\psi(x), \tag{7}$$

which, in the magnetic gauge, yields the dual symmetric field equations as given by,

$$G^{\ \nu}_{\mu\nu,} = F^{\ \nu}_{\mu\nu,} = j_\mu\ \ and\ \ G^{(d)\,\nu}_{\mu\nu,} = B^{\nu}_{\mu\nu,} = k_\mu, \tag{8}$$

and, in fact, has an intimate connection with the color electric flux confinement in QCD. Furthermore, in order to avoid the problems due to point like structure and the singular behavior of the potential associated with monopoles, we use the regular dual magnetic potential ($B_\mu^{(d)}$) for the topological part and introduce a complex scalar field $\phi(x)$ for the monopole. With these considerations, the built-in-dual structure of the Lagrangian (7) may be shown to impart it the flux confining features which becomes more clear if we express it in the quenched approximation as,

$$\pounds_d^{(m)} = -4\pi g^{-1} B_{\mu\nu}^2 + \left| \left[\partial_\mu + i\frac{4\pi}{g} B_\mu^{(d)}\right]\phi \right|^2 - V(\phi). \quad (9)$$

With $V(\phi)$ as a proper effective potential, it induces the dynamical breaking of the magnetic symmetry which leads to the monopole condensation in QCD vacuum and imparts it the (dual) superconducting nature in a way identical to that with Ginzburg-Landau Lagrangian of superconductivity. As a result, the color isocharges are expected to get confined in such magnetically condensed dual QCD vacuum if one takes the effective potential at one-loop level as given by [36],

$$V_{cf}(\phi) = 3(\sqrt{2}\alpha_s)^{-2}\left[\phi_0^4 + (\phi^*\phi)^2\left\{2ln\left((\phi^*\phi)\phi_0^{-2}\right) - 1\right\}\right], \quad (10)$$

(ϕ_0 being the VEV of ϕ) which is extremely reliable in the deep infrared sector of QCD where the couplings are very intense such that $\alpha_s(=g^2/4\pi) \to 1$ and color confinement is strongly enforced. However, since the coupling constant in QCD runs as a result of its asymptotic degree of freedom (in addition to the confinement), its experimentally approachable values lie within far-ultraviolet to near infrared region where the QCD makes a transition from perturbative to non-perturbative phase. Since, in the present case, we are interested in the phase transition study of dual QCD vacuum, the use of an effective potential reliable in relatively weak coupling near-infrared regime is naturally desired and, therefore, we choose the following familiar quadratic potential for inducing the magnetic condensation of QCD vacuum,

$$V_{pt}(\phi) = 3\lambda\alpha_s^{-2}(\phi^*\phi - \phi_0^2)^2. \quad (11)$$

With this potential, the Lagrangian (9) then leads to the field equations given as below;

$$(\partial^\mu - i\sqrt{4\pi\alpha_s^{-1}}B^{(d)\mu})(\partial_\mu + i\sqrt{4\pi\alpha_s^{-1}}B_\mu^{(d)})\phi + 6\lambda\alpha_s^{-2}(\phi^*\phi - \phi_0^2)\phi = 0, \quad (12)$$

$$B_{\mu\nu,}^{\ \ \nu} + i\sqrt{4\pi\alpha_s^{-1}}(\phi^* \overleftrightarrow{\partial}_\mu \phi) - 8\pi\alpha_s^{-1}B_\mu^{(d)}\phi\phi^* = 0. \quad (13)$$

These equations under cylindrical symmetry (ρ, φ, z) alongwith the field ansatz given by,

$$B_\varphi^{(d)} = -B(\rho), B_\rho^{(d)} = B_z^{(d)} = 0 = B_0^{(d)},$$

$$\phi = \chi(\rho)exp(in\varphi), \quad (14)$$

transform to the following form,

$$\frac{1}{\rho}\frac{d}{d\rho}\left(\rho\frac{d\chi}{d\rho}\right) - \left[\left(\frac{n}{\rho} + (4\pi\alpha_s^{-1})^{1/2}B(\rho)\right)^2 + 6\lambda\alpha_s^{-2}\left(\chi^2 - \phi_0^2\right)\right]\chi(\rho) = 0, \quad (15)$$

$$\frac{d}{d\rho}\left[\rho^{-1}\frac{d}{d\rho}\left(\rho B(\rho)\right)\right] - (16\pi\alpha_s^{-1})^{1/2}\left(\frac{n}{\rho} + (4\pi\alpha_s^{-1})^{1/2}B(\rho)\right)\chi^2(\rho) = 0, \quad (16)$$

where, $E_m(\rho) = -\rho^{-1}\frac{d}{d\rho}\left(\rho B(\rho)\right)$ represents the color electric field. For a more convenient representation, we use the dimensionless parameters as,

$$r = 2\sqrt{3\lambda}\alpha_s^{-1}\phi_0\rho, F(r) = (4\pi\alpha_s^{-1})^{\frac{1}{2}}\rho B(\rho),$$

$$H(r) = \phi_0^{-1}\chi(\rho), \quad (17)$$

so that the equations (15) and (16) take a simpler form as,

$$H'' + \frac{1}{r}H' + \frac{1}{r^2}(n+F)^2) + \frac{1}{2}H(H^2-1) = 0, \quad (18)$$

$$F'' - \frac{1}{r}F' - \alpha(n+F)H^2 = 0, \quad (19)$$

where, $\alpha = 2\pi\alpha_s/3\lambda$ and the primes stand for the derivative with respect to r. Using the asymptotic boundary conditions, $F(r) \overset{r\to\infty}{\longrightarrow} -n$, $H \overset{r\to\infty}{\longrightarrow} 1$, the asymptotic solution for $F(r)$ may then be obtained in the following form,

$$F(r) = -n + BrK_1(\sqrt{\alpha}r), \quad (20)$$

where, B is the integration constant and the modified Bessels function $K_1(\sqrt{\alpha}r)$ is, $\sqrt{\frac{\pi}{2\sqrt{\alpha}r}}exp(-\sqrt{\alpha}r)$. On using equation (17), it leads to,

$$F(\rho) = -n + C\sqrt{\rho}\, exp(-m_B\rho), \quad (21)$$

where, $C = 2B\pi(3\sqrt{2}\lambda g^{-3}\phi^0)^{\frac{1}{2}}$ and $m_B = (8\pi\alpha_s^{-1})^{\frac{1}{2}}\phi_0$ is the mass of the magnetic glueballs as vector mode of the magnetically condensed vacuum. Since, the function $F(\rho)$ is associated with the color electric field through gauge potential $B(\rho)$, it shows the emergence of dual Meissner effect and the confinement of the color isocharges in magnetically condensed dual QCD vacuum. Further, the vector-scalar glueball mass ratio as fixed by the effective phenomenological potential (11) given by,

$$\frac{m_B}{m_\phi} = \sqrt{\frac{2\pi\alpha_s}{3\lambda}}, \quad (22)$$

then leads to, $m_\phi = 4\sqrt{3\pi\lambda\alpha_s^{-1}}\phi_0$, as the scalar glueball mass which represents the threshold for magnetic condensation of QCD vacuum. These dual QCD parameters at zero temperatures, in fact, exactly reproduce those obtained using the one-loop effective potential, in the limit $\lambda \to 1$. In

Table 1 The masses of vector and scalar glueball as functions of α_s.

α_s	γ	$\phi_0(GeV)$	$m_B(GeV)$	$m_\phi(GeV)$
0.22	7.891	0.149	1.51	2.22
0.47	6.28	0.167	1.21	1.22
0.96	5.40	0.181	0.929	0.655

addition, the energy per unit length of the associated flux tube configuration governed by the field equations (18) and (19) and the Lagrangian (9), may also be obtained in the following form,

$$k=\gamma\phi_0^2 \text{ with } \gamma=2\pi\int_0^\infty rdr\left[\frac{6\lambda}{g^2}\frac{(F')^2}{r^2}+\frac{(n+F)^2}{r^2}H^2+(H')^2+\frac{(H^2-1)^2}{4}\right]. \quad (23)$$

In view of the relationship of k with Regge slope parameter as given by, $k=(2\pi\alpha')^{-1}$ with $\alpha'=0.90\ GeV^{-2}$, and using the numerical computation of equation (23) for γ in the same way as done with one-loop potential [33, 36], we obtain the vector glueball masses (with the phenomenological effective potential) for some typical values of strong coupling in full infrared sector of QCD at zero-temperature and are given as, The present dual QCD model, therefore, strictly supports a flux-tube configuration and indicates a linear confinement of the color isocharges as a result of the magnetic condensation of QCD vacuum. At moderate couplings, such system has been shown [34, 35] to favor type-II superconducting phase and a number of color flux tubes are expected to be produced as that during the passage of heavy ions in heavy ion collisions which may split thermally resulting in quark-pairs creation. The thermalized system may then switch over to the QGP phase where the non-perturbative properties of QCD vacuum are expected to get largely modified. As such, the estimates presented here may now be utilized (as initial zero temperature parameters) for analyzing the behavior of QCD at finite temperatures and its phase structure.

3 Thermodynamical Variables in Thermal QCD

In view of the enormous potential importance of the study of finite temperature QCD in hadronic world, the thermodynamical properties of QCD are supposed to play an important role to describe the dynamics of different phases of QCD including QGP where one uses the equilibrium thermodynamics to get the properties of such a matter at a very high temperature/density. It leads to a search for the conditions with sufficient energy densities so that the thermodynamical system becomes chemically and thermally equilibrated where thermal and chemical equilibrium indicate that the momenta of the constituent particles are distributed according to equilibrium thermodynamics and the different constituent species are present according to their relative thermodynamic weights respectively. Statistical concepts may then be used for the fireball formed in high energy heavy-ion collisions of large nuclei and the resulting statistical description of different phases in QCD may then be exploited in determining the critical parameters of the phase transitions. The description of such a system involving a large number of particles is suitably done in statistical mechanics, where statistical variables such as energy density ε, entropy density s, pressure P, etc. can be expressed as functions of temperature (T) and finite chemical potential (μ) only. Using the grand canonical ensemble formalism, the partition function for a thermodynamical system, in thermal and chemical equilibrium, may be given by,

$$Z=Tr\left[\exp\left(-\frac{1}{T}(\hat{H}-\mu\hat{N})\right)\right], \quad (24)$$

where, $\hat{H}$ and $\hat{N}$ are the Hamiltonian and the particle number operators respectively and the natural units $(\hbar=c=k=1)$ have been used. The trace in equation (24) implies a summation over all physical states accessible to the system in a spatial volume V and temperature $T=\beta^{-1}$. For simplicity, let us proceed for the single component systems, as the generalization of the treatment to several kinds of particles is straightforward. In the grand canonical ensemble, both the energy and the particle number fluctuate and their average values are expressed as,

$$\varepsilon=\frac{T^2}{V}\frac{\partial}{\partial T}\ln Z+\mu n \quad (25)$$

and

$$n=\frac{T}{V}\frac{\partial}{\partial\mu}\ln Z. \quad (26)$$

Using the particle number representation with equation (24), the resulting expression for the logarithm of the grand canonical partition function of particles and antiparticles with mass m and chemical potential μ and degeneracy factor g in the large volume limit of a free gas, is obtained as,

$$\ln Z(T,\mu,V)=\frac{gV}{6\pi^2T}\int_0^\infty\frac{dkk^4}{(k^2+m^2)^{1/2}}\left[[\exp\{(k^2+m^2)^{1/2}-\mu\}T^{-1}+\eta']^{-1}+[\exp\{(k^2+m^2)^{1/2}+\mu\}T^{-1}+\eta']^{-1}\right], \quad (27)$$

where, $\eta'=+1$ for fermions and -1 for bosons. The first law of thermodynamics expressed as,

$$dE=TdS-PdV+\mu dN, \quad (28)$$

gives the energy as a thermodynamic function of the entropy (S), the volume (V) and the number of particles (N) and may be used for getting entropy and pressure (P). Since, the set of variables (T,V,μ) is more convenient then the set (S,V,N) for the case of varying N, the thermodynamical potential (Ω) with the change of variables may be expressed as,

$$\Omega(T,V,\mu)=E-TS-\mu N. \quad (29)$$

Further, the thermodynamical potential is related to the grand canonical partition function as,

$$\Omega(T,V,\mu) = -T\ln Z. \tag{30}$$

Using equations (28) and (29), the coefficients S, P and N may be given by the partial derivatives of thermodynamical potential as,

$$S = -\left(\frac{\partial\Omega}{\partial T}\right)_{V,\mu},\ P = -\left(\frac{\partial\Omega}{\partial V}\right)_{T,\mu},\ N = -\left(\frac{\partial\Omega}{\partial\mu}\right)_{T,V}. \tag{31}$$

Combining (31) with (30), pressure (P) and the entropy density $s = \frac{S}{V}$ may be expressed as,

$$P = \frac{\partial}{\partial V}(T\ln Z) = \frac{T}{V}lnZ = -\frac{\Omega}{V} \tag{32}$$

and

$$s = \frac{1}{V}\frac{\partial}{\partial T}(T\ln Z). \tag{33}$$

In order to further understand the thermodynamic aspect of the phase transition from hadronic phase to QGP phase, the other associated variables like speed of sound (c_s^2) and specific heat (C_V) also play an important role. The said quantities may be identified by using the conventional thermodynamics as given below,

$$c_s^2 = \frac{dP}{d\varepsilon} = \varepsilon\frac{d(P/\varepsilon)}{d\varepsilon} + \frac{P}{\varepsilon},$$

$$c_s^2 = \frac{s(T)}{C_V(T)}. \tag{34}$$

The speed of sound in a thermodynamical system is, infact, a physical quantity used to characterize the state of a system and is related to the speed of small perturbations produced in thermalized QCD matter. On the other hand, the specific heat at constant volume is defined from the variation of energy density with temperature at constant volume, given as, $C_V = \left(\frac{\partial\varepsilon}{\partial T}\right)_V$, which may also be expressed as,

$$C_V = 4\frac{\varepsilon(T)}{T^4} + \left(\frac{\partial\varepsilon/T^4}{\partial T}\right)_V, \tag{35}$$

which, in the high temperature limit, leads to, $C_V(T)/T^3 \to 4\varepsilon(T)/T^4$.

Furthermore, the momentum integral in (27) may be calculated exactly in both the cases of massless fermions and massless bosons whose chemical potential is zero $(m = \mu = 0)$, and is given in the following form,

$$(T\ln Z)_f = \frac{g_f V}{24}\left(\frac{7}{30}\pi^2T^4 + \mu^2T^2 + \frac{1}{2\pi^2}\mu^4\right), \tag{36}$$

and,

$$(T\ln Z)_b = \frac{g_b V}{90}\pi^2T^4. \tag{37}$$

Let us now consider a gas of quarks with two flavors and gluons. The degeneracy factors in $SU(2)$ QCD case are then, $g_f = 2\times2\times2\times2 = 16$ for quark-antiquark pairs and $g_b = 2\times3 = 6$ for gluons. The grand canonical partition function for the case of free quarks, antiquarks and gluons may be obtained by using equations (36) and (37) and is given by,

$$(T\ln Z)_{q+g} = \frac{2}{3}\left(\frac{\pi^2T^4}{3} + \mu_q^2T^2 + \frac{1}{2\pi^2}\mu_q^4\right)V, \tag{38}$$

where, the chemical potential of u- and d-quarks has been taken to be equal, $\mu_u = \mu_d = \mu_q$. Using equations (26) and (36), the net quark number density may be expressed as,

$$n_q = \frac{4}{3}\left(\mu_qT^2 + \frac{1}{\pi^2}\mu_q^3\right). \tag{39}$$

Similarly, the net baryon number density of a two flavor plasma (with quark baryon number as $\frac{1}{3}$) is given by,

$$n_{Bp} = \frac{4}{9}\left(\mu_qT^2 + \frac{1}{\pi^2}\mu_q^3\right). \tag{40}$$

For, a pion gas with the degeneracy factor of three, equation (37) leads to,

$$(T\ln Z)_\pi \simeq \frac{V}{30}\pi^2T^4. \tag{41}$$

These thermodynamical considerations are, in fact, very much useful for the multi-particle hadronic systems for discussing their thermal evolution, the associated equation of state and the phase structure. For the case of a system of quarks and gluons confined to a finite region of space, let us therefore discuss the thermal evolution of the MIT bag model using the abovementioned considerations alongwith the parameters of dual QCD that may be useful to analyse the hadronic and QGP phase of the matter.

4 MIT Bag Model and Dual QCD Vacuum

In view of the present understanding of the hadron structure, it is reasonable to suppose that the ground state hadrons are spherically symmetric and the quarks shall consequently be confined to a sphere of finite radius. As a result, a model for the hadron has been put forward [37–39], in which a strongly interacting particles consist of fields confined to a finite region of space, identified as a "Bag" which may, in turn, be conveniently used for describing the typical phase structure of QCD. The two features, asymptotic freedom and confinement, of the theory of quarks and gluons (the QCD) may, in fact, be incorporated in the bag model in a crude way: inside the bag, interactions are neglected or are treated in the lowest order perturbation theory; outside the bag, quarks are forbidden to appear as free particles. This last feature is achieved by giving the vacuum a constant finite energy confined to a small regions of space. The hadron energy in its confined phase may, thus, be expressed as,

$$E_h = BV + \frac{C}{R_h}, \tag{42}$$

where, the first part corresponds to the energy associated with the volume of the bag due to the finite energy density of the vacuum, while the second part is the energy due to the kinetic energy of the quarks inside the bag which is proportional to the inverse of the radius of the bag as a consequence of the quantum mechanical uncertainty principle and B represents the bag constant which may be identified by the confining part of the energy expression (23) recalculated after taking the multi-flux tube system as a periodic system on a S^2-sphere [35] and is given as,

$$B^{1/4} = \left(\frac{12}{\pi^2}\right)^{1/4} \frac{m_B}{8}. \tag{43}$$

Minimization of (42), in turn, leads to the effective radius of the hadron bag as derived below,

$$\frac{\partial E_h}{\partial R_h} = 4\pi R_h^2 B - \frac{C}{R_h^2} = 0, \tag{44}$$

which gives,

$$R_h = \left(\frac{C\pi}{3}\right)^{1/4} \frac{4}{m_B}. \tag{45}$$

Using expression (42), the force per unit area leads to the radial pressure on the bag surface, which may be obtained as,

$$P = -\frac{\left(\frac{\partial E_h}{\partial R_h}\right)}{4\pi R_h^2} = -B + \frac{C}{4\pi R_h^4}. \tag{46}$$

For a static bag, the radial pressure on the bag surface vanishes and the bag constant acts as a restoring force to equilibrate the pressure generated by the kinetic energy of quarks inside the bag. Since the bag model has been used to describe the quark-gluon matter not only inside the hadrons but also in any enclosed finite volume, let us assume that the whole quark matter is enclosed inside a big bag, so that the ground state shift from the physical vacuum into the QCD vacuum inside the bag is achieved by adding a term $(\ln Z)_{vac} = -\frac{BV}{T}$ to the equation (38). For simplicity, let us restrict ourselves to the non-strange hadrons (pions) and quarks (u and d). In the case of a plasma of non-interacting quarks and gluons, using (36) and (37), the grand canonical partition function for QGP, is then given by,

$$(T\ln Z)_p = \frac{2}{3}V\left(\frac{7}{30}\pi^2T^4 + \mu_q^2T^2 + \frac{1}{2\pi^2}\mu_q^4\right) + \frac{\pi^2}{15}VT^4 - BV, \tag{47}$$

where, the index p refers to the plasma phase. Thus, the equation of state for the phenomenological bag model in its plasma phase, may be obtained by using equations (25) and (32) which leads to the expressions for the energy density and plasma pressure as given below,

$$\varepsilon_p = \frac{2}{3}\pi^2T^4 + 2\mu_q^2T^2 + \frac{\mu_q^4}{\pi^2} + B \tag{48}$$

and

$$P_p = \frac{2}{9}\pi^2T^4 + \frac{2}{3}T^2\mu_q^2 + \frac{\mu_q^4}{3\pi^2} - B, \tag{49}$$

where, the quark masses and the perturbative QCD interactions are neglected. The energy density and the pressure then satisfy the following relationship,

$$P_p = \frac{1}{3}(\varepsilon_p - 4B). \tag{50}$$

Further, the equations (26) and (40) lead to the baryon number density given as,

$$n_{Bp} = \frac{4}{9}\left(\mu_qT^2 + \frac{1}{\pi^2}\mu_q^3\right), \tag{51}$$

which remains unaltered by bag dynamics. Use of such thermodynamical concepts for the equation of state for the different phases of hadronic matter including the QGP phase, then plays a crucial role in identifying the detailed phase structure of QCD, the dynamics of phase transitions and extracting the critical parameters associated with the different phase transitions expected in the hadronic world.

5 Dynamics of Phase Transition

One of the most exciting features of the thermal QCD is its ability to predict a phase transition at some critical temperature (T_c) and critical baryon chemical potential (μ_c) to a new phase of weakly bound quarks and gluons, viz. the Quark-Gluon Plasma (QGP) phase. In order to, understand the formation and characteristics of such new phase in terms of the associated critical parameters, let us use the Gibbs criteria according to which the pressure, temperature and chemical potentials must remain constant across the phase boundary and, therefore, the equilibrium conditions for two phases consisting of identical particles are the equalities of the temperature, chemical potential and pressure in both the phases [40]. Assuming N_q quarks more than antiquarks and N_N nucleons more than anti-nucleons, the conservation of the total baryon number $(\frac{1}{3}N_q + N_N = constant)$ yields,

$$\frac{\partial N_q}{\partial N_N} = -3. \tag{52}$$

The differential change in Gibbs free energy, $G(T,P,N) = E - TS + PV$ when used with the equation (28), may be used to get a relation between the chemical potentials of quarks and nucleons in the following form,

$$\left(\frac{\partial G}{\partial N_q}\right)_{T,P} = \mu_q, \text{ and } \left(\frac{\partial G}{\partial N_N}\right)_{T,P} = \mu. \tag{53}$$

Further, the minimization of the Gibbs free energy at fixed temperature and pressure alongwith the equation (52), leads,

$$0 = \frac{\partial G}{\partial N_N} + \frac{\partial G}{\partial N_q}\frac{\partial N_q}{\partial N_N} = \frac{\partial G}{\partial N_N} - 3\frac{\partial G}{\partial N_q}, \tag{54}$$

which, in view of the equation (53) yields, $\mu = 3\mu_q$. With these considerations, the phase equilbrium condition for the matter in hadronic (h) and plasma (p) phases may be expressed as the Gibbs criteria given by,

$$P_h = P_p = P_c;\ T_h = T_p = T_c;\ \mu = 3\mu_q = \mu_c, \tag{55}$$

c representing the critical point of QGP-phase transition. As such, for the study of phase diagram of dense and hot hadronic matter for a equilibrium phase transition, let us first consider the transition in the case where $\mu_q = 0$. At low temperatures, this baryon free matter is composed of the lightest mesons, i.e. mostly the pions and for simplicity, we use an approximation by treating the pion as a massless particle. At very high temperatures, we consider the hadronic matter composed only of quarks-antiquarks (in equal numbers) and gluons, forming a quark-gluon plasma. In both the high temperature and the low temperature phases, their interactions are neglected (except for the bag-constant). The description of the transition is, therefore, expected to be dominated by entropy considerations and counting the degrees of freedom. Using (41) alongwith equations (25) and (32), the energy density and the pressure for a gas of massless pions may be expressed in the following form,

$$\varepsilon_\pi = 3 \times \frac{\pi^2}{30} T^4 \tag{56}$$

and

$$P_\pi = 3 \times \frac{\pi^2}{90} T^4, \tag{57}$$

where, the factor of 3 accounts for the three pionic degrees of freedom $(\pi^{\pm,0})$. The entropy density (33) for pions is then given by,

$$s_\pi = 2 \times \frac{\pi^2}{15} T^3. \tag{58}$$

The energy density, pressure, entropy density, speed of sound and specific heat of the quark-gluon plasma given by equations (48), (49), (33), (34) and (35) respectively, may then be expressed as,

$$\varepsilon_p = \frac{2}{3}\pi^2 T^4 + B, \tag{59}$$

$$P_p = \frac{2}{9}\pi^2 T^4 - B, \tag{60}$$

$$s_p = 2 \times \frac{4}{9}\pi^2 T^3, \tag{61}$$

$$c_s^2 = \frac{1}{3}\frac{(2\pi^2 T^4 - 9B)}{(2\pi^2 T^4 + 3B)} \tag{62}$$

and

$$C_V = \frac{8\pi^2 T^3}{3}\frac{(2\pi^2 T^4 + 3B)}{(2\pi^2 T^4 - 9B)}. \tag{63}$$

The baryon number density $n_{Bp}(\mu_q = 0)$ vanishes for the mesons. Using the Gibbs criteria for phase transition as given by equation (55), the phase crossover may be discussed as a function of the temperature and, therefore, equating P_p and P_π then leads to a phase transition temperature given by,

$$T_{c(\pi)}^{QGP} = \left(\frac{90}{17\pi^2}\right)^{1/4} B^{1/4} \approx 0.856 B^{1/4}. \tag{64}$$

In order to extend these considerations to the domain of non-zero chemical potential, let us undertake the case of matter with finite baryon density and restrict ourself, for simplicity, to the system of nucleons only. Hence, using the expression (36) with the degeneracy factor $g_f = 2 \times 2$ for nucleons, the nucleon pressure may be expressed as,

$$P_N = \frac{1}{6}\left(\frac{7}{30}\pi^2 T^4 + \mu_q^2 T^2 + \frac{1}{2\pi^2}\mu_q^4\right). \tag{65}$$

The associated baryon density (n_{Bp}) with non-zero chemical potential is given by expression (51). The co-existence of two phases as per Gibbs criteria given by equation (55), then leads to the occurrence of a phase transition at a typical temperature. Hence, equating nucleon pressure and plasma pressure given by equations (65) and (49) respectively, we get,

$$\frac{11}{60}\pi^2 T^4 + \frac{1}{2}\mu_q^2 T^2 + \frac{1}{4\pi^2}\mu_q^4 = B. \tag{66}$$

In the transition region, for the phase transition at a critical point $(\mu_q = \frac{\mu_c}{3}, T = T_c)$ it leads,

$$\frac{11}{10}\pi^2 T_c^4 + \frac{1}{3}\mu_c^2 T_c^2 + \frac{1}{54\pi^2}\mu_c^4 = 6B. \tag{67}$$

However, with the increase of the temperature, the nucleons density drops down as a result of the reduction in the chemical potential and the phase transition occurs at a critical temperature where the nucleons start disappearing forcing the chemical potential to vanish. Hence, the expression (67), under such conditions leads to the critical temperature given as,

$$T_{c(N)}^{QGP} = \left(\frac{60}{11\pi^2}\right)^{1/4} B^{1/4} \approx 0.862 B^{1/4}, \tag{68}$$

which is in close agreement with that given by equation (64). The critical temperature $(T_{c(N)}^{QGP})$, infact, is a fundamental quantity of interest as it serves to parametrize the temperature at which the confined and the weakly bound/deconfined phases are expected to coexist.

Furthermore, in addition to the seemingly well behaved nature of QCD in perturbative sector, the complicated infrared structure of QCD is expected to play an important role for the QCD thermodynamics also especially at high temperatures. The non-perturbative modifications of the low momentum spectrum are then definitely expected to be responsible for the substiantial part of the deviations of the equation of state from ideal gas behavior expressible by, $\varepsilon = 3P$ where the leading gas term is eliminated in the difference $\varepsilon - 3P$. Since, this quantity may be extracted from the

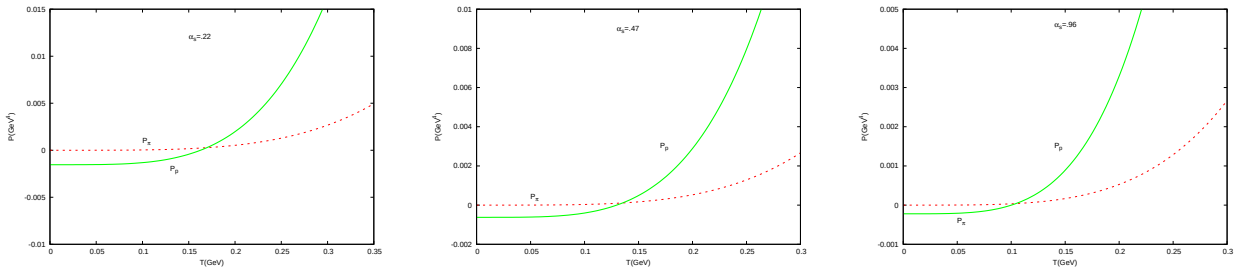

Fig. 1 The variation of plasma pressure and pion pressure with temperature in the infrared sector of QCD for $\alpha_s = 0.22$, $\alpha_s = 0.47$, $\alpha_s = 0.96$.

trace of energy-momentum tensor and the infrared physics is basically responsible for its departure from the ideal gas behavior near the phase transition, it is identified as "trace anomaly" which, infact, measures interactions still present in the medium. It is further linked with an another quantity, viz. "the conformal measure", which, infact, determines the strength of such interactions and turn out to be an important parameter around phase boundary indicating the non-conformal nature of the plasma. Hence, using equation (59) and (60), the associated normalized dimensionless interaction measure($\triangle(T)$) and conformal measure($\mathscr{C}$) may be expressed as,

$$\triangle(T) = \frac{\varepsilon_p - 3P_p}{T^4} = \frac{4B}{T^4} \tag{69}$$

and

$$\mathscr{C} = \frac{\varepsilon_p - 3P_p}{\varepsilon_p} = \frac{4B}{\varepsilon_p}, \tag{70}$$

which certainly needs to be investigated for understanding the dynamics of phase transition around T_c and has been pursued in the next section.

6 Numerical Estimation of Phase Transition Parameters and Implications for QGP

The various thermodynamic factors associated with the bag model in dual QCD discussed in previous section, in fact, play an important role in identifying the phase structure of QCD especially in the context of its QGP phase. The two cases discussed were those associated with the vanishing chemical potential (pion case) and the non-vanishing chemical potential (the nucleon case) which lead to an estimate for the phase transition temperature when the hadronic system transits to the QGP phase.

In order to numerically compute the transition temperature for the case of pions, the pion pressure and associated plasma pressure given by equations (57) and (60) respectively, have been plotted in figure 1 for three different couplings in infrared sector of QCD. Following Gibbs criteria of phase transition with figure 1, leads to the point of QGP phase transition at the critical temperatures of $0.169GeV$, $0.135GeV$ and $0.104GeV$ for the case of $\alpha_s = 0.22, 0.47$ and 0.96 respectively. The same critical temperature may also be computed analytically using equation (62) alongwith equation (43) for bag constant and the values of glueball masses as obtained in terms of table 2, which are in complete agreement with the abovementioned values. In an identical way, the same analysis may be extended to the case of baryons (nucleons) with non-zero chemical potential by using the equation (65) to plot chemical potential with temperature which has been given as figure 2. It leads to the critical temperature of QGP-phase transition corresponding to the points of vanishing chemical potential which implies the vanishing baryon density according to equation (51). Thus, the critical temperatures in infrared sector of QCD for the present case as obtained by figure 2 are; $0.171GeV$, $0.136GeV$ and $0.105GeV$ for $\alpha_s = 0.22$, 0.47 and 0.96 respectively. The analytical values for the critical temperature in the present case may also be calculated using the expression given by equation (66) and a remarkable agreement for the values of the critical temperatures of QGP phase transition among these values is reflected in the present case also. The critical temperatures for QGP phase transition computed for the abovementioned two cases also show a close agreement, in general. These estimations for the critical temper-

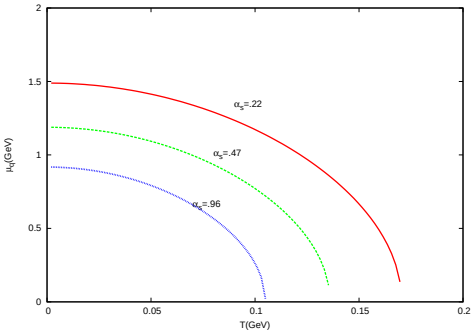

Fig. 2 The variation of chemical potential with temperature in the infrared sector of QCD for $\alpha_s = 0.22$, $\alpha_s = 0.47$, $\alpha_s = 0.96$.

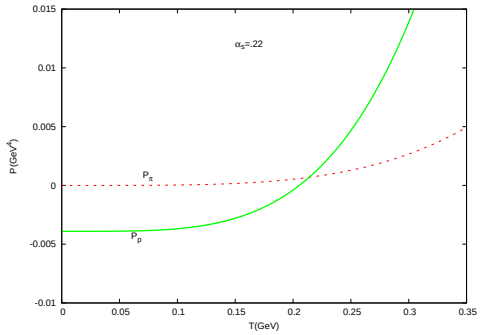

Fig. 3 The variation of plasma pressure and pion pressure with temperature in the infrared sector of QCD with $\alpha_s = 0.22$ for heavy bag ($B^{1/4} = 0.250GeV$).

Table 2 The estimation of critical temperatures for the $\lambda\phi^4$ effective potential with dual QCD for different values of strong coupling constants in infrared sector of QCD.

α_s	$T_{c(\pi)}^{QGP}(GeV)$	$T_{c(N)}^{QGP}(GeV)$	$T_d(GeV)$
0.22	0.169	0.171	0.268
0.47	0.135	0.136	0.221
0.96	0.104	0.105	0.174

atures have been performed using the glueball masses computed using $\lambda\phi^4$ effective-potential for magnetic symmetry breaking in dual QCD. On the other hand, use of a heavy bag (with bag constant $B^{1/4} = 0.250GeV$) leads to the pressure variation as given by figure 3 which, infact, leads to a strong interplay between quark-gluon and hadronic degrees of freedom at the critical temperature as it leads to a critical temperature of $0.214GeV$ which is much above the best fit of lattice results ($T_c = 0.170GeV$) and shifts more towards the complete deconfinement phase ($T_d = 0.268GeV$)[32] of the hadronic matter. All of these estimates have been summarized in table 2. The range of the temperatures thus obtained may then be used to analyse the phase boundaries of QGP phase transition and the deconfinement phase transition in dual QCD.

Furthermore, in view of the expected liberation of quarks and gluons as a result of a possible phase transition around T_c, the energy variations also play an important role to identify the associated change in degrees of freedom in the medium. Figure 4 represents the variation of such normalized energy density for pion and QGP phases with temperature as given by equations (56) and (59) respectively, for different values of strong coupling in the infrared sector of QCD. It has been observed that the energy density increases abruptly at the phase transition temperature and is supplemented by a finite jump (discontinuity) indicating a rapid rise in the degree of freedom in the system. The extent of such discontinuity in the energy density, is identified as the latent heat and may be expressed as,

$$\triangle\varepsilon = \varepsilon_{QGP}(T_c) - \varepsilon_{\pi}(T_c) = 4B, \tag{71}$$

so that it is determined completely by the bag pressure and is a measure of the level difference between the physical and the colored quark-gluon vacuum. The finite discontinuity in energy density at the transition point thus indicates a first-order phase transition and the numerical value of $\Delta\varepsilon$ for vanishing chemical potential comes out to be $0.77GeV/fm^3$, $0.31GeV/fm^3$ and $0.11GeV/fm^3$ for three different couplings, $\alpha_s = 0.22$, $\alpha_s = 0.47$ and $\alpha_s = 0.96$ respectively in the infrared sector of QCD. The value of $\triangle\varepsilon/T^4$ at T_c found to be around 7.5 from figure 4 , is also in close agreement with that calculated analytically.

Keeping in view the fact that the change in equation of state and the speed of sound may have important consequences in the flow properties of the exotic medium (QGP), the variation of the squared speed of sound has been depicted in figure 5(a) using equation (62) for $\alpha_s = .22$, $\alpha_s = .47$ and $\alpha_s = 0.96$ values of coupling. It has been found that in the vicinity of the phase transition near-T_c region the energy density increases much more rapidly than the pressure which makes matter "soft" as indicated by the corresponding plots of pressure and energy density figure 4 and the point where c_s^2 drops to its minimum may be identified as the "softest point". In the QGP phase, c_s^2 then rises with the increase in temperature and approaches to the value $c_s^2 = 0.33$, for all the couplings in infrared sector of QCD, which is close to that in case of the ideal relativistic gas. c_s^2 is then relevant for the dynamical properties of the system and gives a peculiar measure for the deviation from the conformal behavior since, for a conformal symmetric system the speed of sound squared is equal to 1/3 and therefore deviation from this numerical value indicates the breaking of conformal symmetry.

In addition, as an another measure of thermodynamical (energy) fluctuations for the QGP system typically near T_c, the specific heat plays an important role and offers a direct test of the relevance of the conformal symmetry to finite temperature QCD. Figure 5(b), therefore, represents the plot for the normalized specific heat at constant volume using equation (63) for three different couplings in the infrared sector of QCD, which clearly demonstrates the sudden changes in specific heat with a sharp peak around T_c converging very well to $4\varepsilon/T^4$ at high temperatures and indicates the onset of a phase transition. Furthermore, in order to identify the interactions still present in the medium above the critical temperature due to the expected rapid increase in the additional degrees of freedom carried by quark and gluons, the behavior of trace anomaly has been shown in figure 6. Using equation (69) the normalized trace anomaly has been depicted in figure 6(a) for various strong couplings in

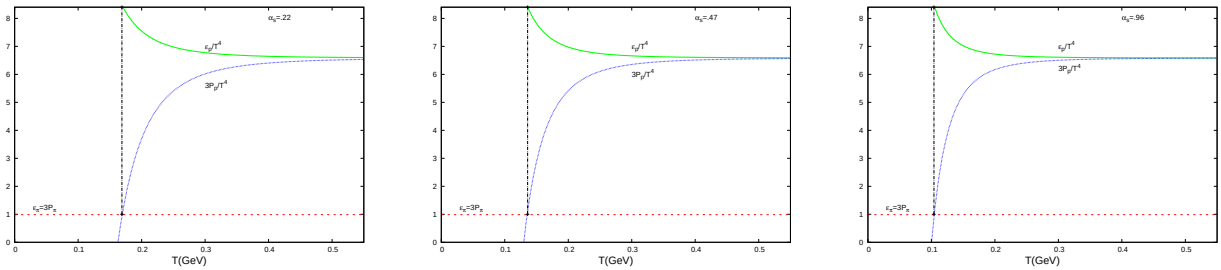

Fig. 4 The variation of normalized energy density for pion and plasma phases with temperature in the infrared sector of QCD for $\alpha_s = 0.22$, $\alpha_s = 0.47$, $\alpha_s = 0.96$.

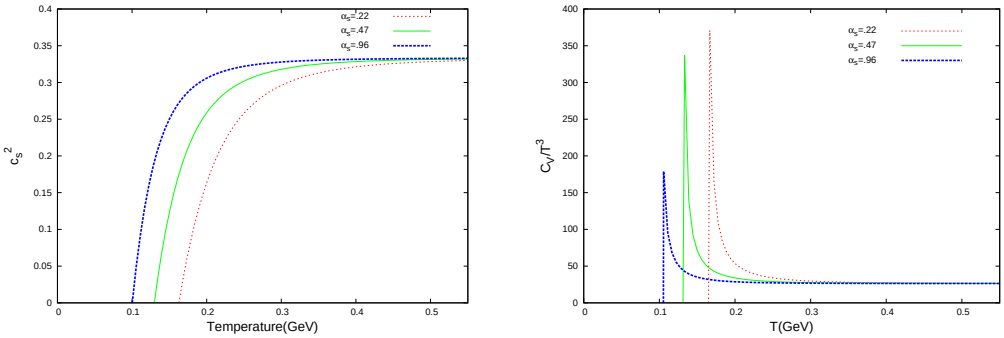

Fig. 5 The variation of squared speed of sound (a) and the normalized specific heat (b) with temperature in the infrared sector of QCD for $\alpha_s = 0.22$, $\alpha_s = 0.47$, $\alpha_s = 0.96$.

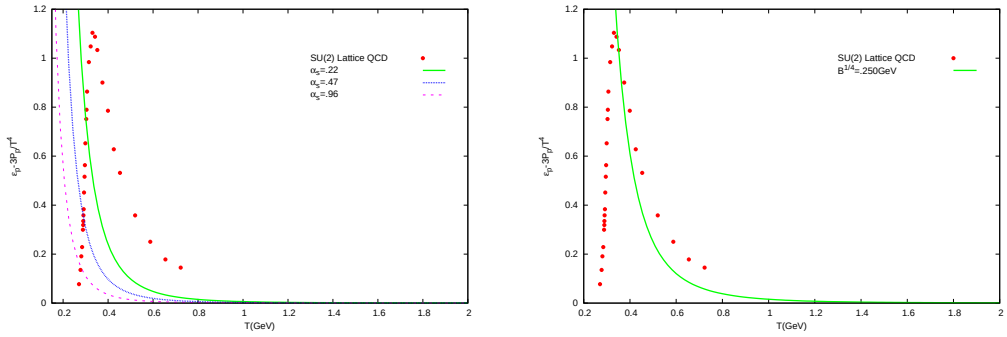

Fig. 6 The variation of interaction measure with temperature in the infrared sector of QCD for (a) $\alpha_s = 0.22$, $\alpha_s = 0.47$, $\alpha_s = 0.96$ and (b) heavy bag ($B^{1/4} = 0.250GeV$).

infrared sector of QCD and in the figure 6(b) for the case of a heavy bag ($B^{1/4} = 0.250GeV$). The corresponding plots for the available SU(2) lattice[16] data with coupling $\alpha_s = 0.11$ have also been depicted for the purpose of comparison. The steep increase in interaction measure near T_c and a subsequent large reduction at high temperature ($T \gg T_c$) is evident from these variations and such behavior is in agreement with that of the lattice studies. The trace anomaly profile in figure 6(b) (for heavy bag), infact, corresponds to the case of near infrared sector of QCD around $\alpha_s \sim 0.11$ (the lattice value) where the vector glueballs appear more massive and the trace anomaly shows a more closer agreement. The high temperature behavior of QGP medium thus seems to be more conformal (scale-invariant). Since, the generation of a scale and the subsequent breaking of conformal invariance at short distances in QCD is quantified by the β-function of QCD, while that at large distance, in the finite temperature plasma by the conformal measure $\mathscr{C}$, this is a relevant

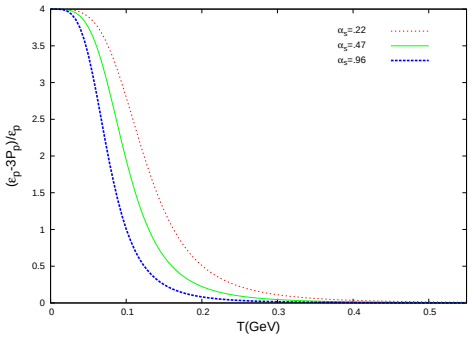

Fig. 7 The variation of conformal measure with temperature in the infrared sector of QCD for $\alpha_s = 0.22$, $\alpha_s = 0.47$, $\alpha_s = 0.96$.

quantity for determining and measuring the deviation of the system from the conformal symmetric system. Hence, using equation (70), the thermal response of conformal measure has been shown in figure 7 which indicates a peak at low temperature and then a monotonous decrease in $\mathscr{C}$ till it vanishes completely at higher temperature ($T \gg T_c$). As such, in the high temperature regime, the present effective theory definitely reproduces the results of thermal QCD at large-distance scales and stands close to a conformal theory.

7 Summary and Conclusions

Using the statistical concepts of basic thermodynamics, the thermal description of dual QCD has been presented in terms of bag model of hadrons and analysed for the quark-gluon plasma phase of hadronic matter. Starting from the partition function of the grand canonical ensemble formalism, given by equation (24), the thermodynamical potential is constructed as given by equation (30) which, in turn, leads to the physically realizable thermodynamical variables given by equations (31)-(35). The thermodynamical potential for fermions and bosons has been calculated in terms of equations (36) and (37) which has been used for its description for mesonic and baryonic cases of hadrons. Constructing the bag model for hadrons using the confining part of the energy in dual QCD formulation, the hadron energy is given by equation (42) which includes the quark kinetic energy alongwith the confining contribution. It has been used to derive the effective radius of the bag and the radial pressure on the bag surface which depend on the vector glueball masses of magnetically condensed QCD vacuum as shown by equations (45) and (46). Constructing the grand canonical partition function for the QGP of non-strange hadrons in terms of equation (47), the energy density and the plasma pressure have been derived in terms of equations (48) and (49) respectively which have been used to deal with the dynamics of the QGP phase transition. With the plasma and hadron pressure in hand, the Gibbs criteria given by equation (55) has been used to compute the transition temperatures as the criteria gives a phase boundary where the system retains the state of minimum thermodynamical potential. Application of these considerations to the simplest system of pions (mesonic system), for which the energy density, pressure and entropy density have been derived in terms of equations (56)-(58) in hadronic phase and (59)-(61) in plasma phase, has been shown to lead to the expression for the transition temperature given by equation (64) from hadronic (mesonic) to QGP phase. The values of transition temperature have then been obtained by graphical plots of equations (57) and (60) as in figure 1 for different couplings in infrared sector of QCD ($0.169GeV, 0.135GeV, 0.104GeV$ for $\alpha_s = 0.22, 0.47$ and 0.96 respectively) and these values are in good agreement with those obtained analytically by expression given by equation (64). In an identical way, the analysis has been extended to the case of baryons with finite chemical potential for which the hadron pressure is given by equation (65) and the equality of (65) with (49) (the associated plasma pressure) as per Gibbs-criteria leads to equation (67). The plot of equation (67) given by figure 2, leads to the critical temperatures ($0.171GeV, 0.136GeV, 0.105GeV$ for $\alpha_s = 0.22, 0.47, 0.96$ respectively) in full infrared sector of QCD. Identical values of critical temperature of QGP phase transition are obtained by the corresponding analytical expression given by equation (68) as in the pionic case. All of these critical temperature values have been summarized in table 2. It suggests that, when observed collectively, in the physically accessible near infrared region of QCD ($\alpha_s = 0.22$), the range of temperatures for QGP phase transition is expected to be $0.169GeV - 0.268GeV$ and the hadronic system goes over to the completely deconfined phase at $0.268GeV$ in this region. The system in between may relax through a mixed phase of QGP and hot hadron gas. Moreover, the normalized energy density profiles depicted in figure 4 in full infrared sector of QCD, show an abrupt increase at the transition point and a large amount of latent heat has been shown to be generated which is indicative of the onset of a first order phase transition. As a result, the generation of such large amount of latent heat may be associated with a possible signal of QGP as it may appear as a shock wave given off at the phase transition. Similar conclusions may also be drawn from the consideration of the specific heat at constant volume in figure 5(b) which shows a steep rise near phase transition (like the lambda transition in liquid Helium) and acts as a measure of large energy fluctuations near T_c. Such measurements of C_V are also directly related to the event-by-event transverse momentum fluctuations in heavy-ion collision experiments[41, 42]. In an identical way, the squared speed of sound has also been shown as an another measure of thermodynamical fluctuations in terms of a kinetic variable. As shown in figure 5(a), c_s^2 shows very sharp

variations around T_c, decreasing rapidly below T_c and rising steeply around T_c mainly due to the rapid increase in energy density making the matter soft around the critical point. It then reaches to its maximum at very large temperatures where the system turns almost an ideal one. A smaller speed of sound (below T_c), infact, imply a slower flow for the finite size systems created in the heavy-ion collision events. The change in the equation of state and the speed of sound may thus have important consequences in the flow properties of QGP created in heavy-ion collision experiments. As such, the speed of sound definitely governs the evolution of fire-ball produced in these experiments and plays a crucial role in the associated hydrodynamic formulation of the QGP where the elliptic flow [43, 44](for example), appearing as one of the important measure for the QGP signatures, becomes highly sensitive to the value of the speed of sound. Furthermore, using equation (69), the graphical representation of trace anomaly in figure 6 has been shown to lead to the very large values of interaction measure close to the transition temperature meaning thereby that the QGP at such temperatures remains far from the conformal limit. It is also evident that there are considerable interaction effects in the temperature range, $1 \leq T/T_c \leq (2-3)$. It may, therefore, be conjectured that the form of trace anomaly is, infact, a consequence of the critical behavior of the theory and the functional behavior of trace anomaly (with pressure containing most of the interaction effects) might have its links with the difference between the chromomagnetic and chromoelectric contributions. However, the question of its detailed behavior in the transition region, the origin of the deviations from ideal gas form and the appearance of additional degrees of freedom still remain open. In an identical way, the graphical plot in figure 7 for the conformal measure given by equation (70) also demonstrates the breakdown of the conformal symmetry for the temperatures, $T \leq T_c$ due to quantum anomalies and evolution of additional degrees of freedom and the subsequent appearance of a scale responsible for large trace anomaly also. Figure 5 and 7 further demonstrate that the conformal measure and squared speed of sound reflect just opposite behavior (lower the value of $\mathscr{C}$, higher is the value of c_s^2 and vice-versa) which is an indication that the conformal measure clearly appears as a measure of the strength of the interaction in the system. As such, the study of the dynamical variables mentioned above is of extreme importance in the description of the hydrodynamical expansion of hot hadronic matter which has the direct physical relevance to the various ongoing experiments of relativistic heavy-ion collisions and may, therefore, lead to a new window to observe the QGP and the deconfined phases of hadronic matter in the experimentally realizable near infrared region of QCD.

Acknowledgements The authors HCC and GP are thankful to the University Grants Commission, New Delhi (India) for the financial support in terms of the grant no. 41/840/2012(SR) during the course of the study.

References

1. I. Arsene, I. G. Bearden, D. Beavis et al., Nucl. Phys. **A757**, 1 (2005).
2. K. Adcox, S. S. Adler, S. Afanasiev et al., Nucl. Phys. **A757**, 184 (2005).
3. J. Adams, M. M. Aggarwal, Z. Ahammed et al., Nucl. Phys. **A757**, 102 (2005).
4. K. Aamodt, A. A. Quintana, D. Adamova et al., Phys. Rev. Lett. **106**, 3032301 (2011).
5. K. Aamodt, A. A. Quintana, D. Adamova et al., Phys. Lett. **B696**, 30-39 (2011).
6. K. Aamodt, B. Abelev, A. A. Quintana et al., Phys. Rev. Lett. **105**, 252302 (2010).
7. B. Müller, *Particle Production in Highly Excited Matter ed. H. Gustbrod and J. Rafelski*, (Plenum Press, New York, 1993).
8. E. Shuryak, Prog. Part. Nucl. Phys. **62**, 48 (2009).
9. B.Müller, J. Schukraft and B. Wyslouch, Ann. Rev. Nucl. Part. Sci. **62**, 361 (2012).
10. D. J. Gross, R. Pisarski and L. Yatti, Rev. Mod. Phys. **53**, 43 (1981).
11. F. Karsch, Journal of Physics **G35**, 104096 (2008).
12. M. Cheng, S. Ejiri, P. Hegde et al., Phys. Rev. **D81**, 054504 (2010).
13. Y. Aoki, G. Endrődi, Z. Fodor, S. D. Katz, and K. K. Szabó, Nature **443**, 675 (2006).
14. Z. Fodor, Journal of Physics: Conference Series **230**, 012013 (2010) .
15. Y. Aoki, S. Borsányi, S. Durr et al., Nucl. Phys. **A830**, 1 (2009).
16. J. Engels, J. Fingberg, K. Redlich, H. Satz, M. Weber, Z. Phys. C- Particles and Fields **42**, 341 (1989).
17. M. Gyulassy, L. McLerran, Nucl. Phys. **A750**, 30 (2005).
18. Sz. Borsányi, G. Endrődi, Z. Fodor, S. D. Katz, S. Krieg, C. Ratti, K. K. Szabó, JHEP **08**, 053 (2012).
19. C. P. Singh, Phys. Rep. **236**, 147 (1993).
20. B. Müller, Rep. Prog. Phys. **58**, 611 (1995).
21. J. Cleymans, R. V. Gavai and E. Suhonen, Phys. Rep. **130**, 217 (1986).
22. K. S. Lee, M. J. Rhoades-Brown and U. Heinz, Phys. Rev. **C37**, 1452 (1988).
23. P. R. Subramanian, H. Stocker and W. Greiner, Phys. Lett. **B173**, 468 (1986).
24. K. Redlich, Z. Phys. **C27**, 633 (1985).
25. T. Matsui, B. Svetitsky and L. D. McLerran, Phys. Rev. **D34**, 2047 (1986).

26. N. Glendenning and J. Rafelski, Phys. Rev. **C31**, 832 (1985).
27. C. P. Singh, P. K. Srivastava, S. K. Tiwari, Phys. Rev. **D80**, 114508 (2009).
28. P. K. Srivastava and C. P. Singh, Int. J. Mod. Phys. **A28**, 1350051 (2013).
29. A. Leonidov, K. Redlich, H. Satz, E. Suhonen and G. Weber, Phys. Rev. **D50**, 4657 (1994).
30. B. K. Patra and C. P. Singh, Phys. Rev. **D54**, 3551 (1996).
31. P. K. Srivastava, S. K. Tiwari and C. P. Singh, Phys. Rev. **D82**, 014023 (2010).
32. H.C. Chandola and D. Yadav, Nucl. Phys. **A829**, 151 (2009).
33. Y.M. Cho, Phys. Rev. **D21**, 1080 (1980); ibid **D23**, 2415 (1981), Y.M. Cho and P.S. Jang, Phys. Rev. **D12**, 3789 (1975).
34. H.C. Pandey and H.C. Chandola, Phys. Lett. **B476**, 193 (2000).
35. H.C. Chandola, D. Yadav, H.C. Pandey and H. Dehnen, Int. Jour. Mod. Phys. **A20**, 2743 (2005).
36. S. Coleman and E. Weinberg, Phys. Rev. **D7**, 1888 (1973).
37. F. E. Close, *An Introduction to Quarks and Partons*, (Academic Press Printed in Great Britain, 1982).
38. A. Hosaka and H. Toki, Phys. Rep. **277**, 65 (1996).
39. A. Chodos, R. L. Jaffe, K. Johnson, C. B. Thorn and V.F. Weisskopf, Phys. Rev. **D9**, 3471 (1974).
40. L. D. Landau and E. M. Lifshiftz, *Course of Theoretical Physics Vol.* 5*, Statistical Physics*, (Pergamon Press, Oxford, 1978).
41. M. Gaździcki et al., Phys. Lett. **B585**, 115 (2004).
42. P. Bożek and W. Broniowski, Phys. Rev. **C85**, 044910 (2012).
43. R. Snellings, New J. Phys. **13**, 055008 (2011) .
44. O. Linnyk, V. P. Konchakovski, W. Cassing and E. L. Bratovskaya, Phys. Rev. **C88**, 034904 (2013).